The hidden anatomy of paranasal sinuses reveals biogeographically distinct morphotypes in the nine-banded armadillo (*Dasypus novemcinctus*)

Guillaume Billet [Corresp., 1], **Lionel Hautier** [2, 3], **Benoit de Thoisy** [4, 5], **Frédéric Delsuc** [2]

[1] Sorbonne Universités, CR2P, UMR 7207, CNRS, Université Paris 06, Museum national d'Histoire naturelle, Paris, France

[2] Institut des Sciences de l'Evolution, UMR 5554, CNRS, IRD, EPHE, Université de Montpellier, Montpellier, France

[3] Mammal Section, Life Sciences, Vertebrate Division, The Natural History Museum, London, United Kingdom

[4] Institut Pasteur de la Guyane, Cayenne, French Guiana

[5] Association Kwata, Cayenne, French Guiana

Corresponding Author: Guillaume Billet
Email address: guillaume.billet@mnhn.fr

Background. With their Pan-American distribution, long-nosed armadillos (genus *Dasypus*) constitute an understudied model for Neotropical biogeography. This genus currently comprises seven recognized species, the nine-banded armadillo (*D. novemcinctus*) having the widest distribution ranging from Northern Argentina to the South-Eastern US. With their broad diversity of habitats, nine-banded armadillos provide a useful model to explore the effects of climatic and biogeographic events on morphological diversity at a continental scale.

Methods. Based on a sample of 136 skulls of *Dasypus* spp. belonging to six species, including 112 specimens identified as *D. novemcinctus*, we studied the diversity and pattern of variation of paranasal cavities, which were reconstructed virtually using µCT-scanning or observed through bone transparency.

Results. Our qualitative analyses of paranasal sinuses and recesses successfully retrieved a taxonomic differentiation between the traditional species *D. kappleri*, *D. pilosus* and *D. novemcinctus* but failed to recover diagnostic features between the disputed and morphologically similar *D. septemcinctus* and *D. hybridus*. Most interestingly, the high variation detected in our large sample of *D. novemcinctus* showed a clear geographical patterning, with the recognition of three well-separated morphotypes: one ranging from North and Central America and parts of northern South America west of the Andes, one distributed across the Amazonian Basin and central South America, and one restricted to the Guiana Shield.

Discussion. The question as to whether these paranasal morphotypes may represent previously unrecognized species is to be evaluated through a thorough revision of the *Dasypus* species complex integrating molecular and morphological data. Remarkably, our recognition of a distinct morphotype in the Guiana Shield area is congruent with the recent discovery of a divergent mitogenomic lineage in French Guiana. The inflation of the second medialmost pair of caudal frontal sinuses constitutes an unexpected morphological diagnostic feature for this potentially distinct species. Our results demonstrate the benefits of studying overlooked internal morphological structures in supposedly cryptic species revealed by molecular data. It also illustrates the under-exploited potential of the highly variable paranasal sinuses of armadillos for systematic studies.

The hidden anatomy of paranasal sinuses reveals biogeographically distinct morphotypes in the nine-banded armadillo (*Dasypus novemcinctus*)

Guillaume BILLET[1], Lionel HAUTIER[2,3], Benoit de THOISY[4,5], and Frédéric DELSUC[2]

[1]Sorbonne Universités, CR2P, UMR 7207, CNRS, Université Paris 06, Muséum national d'Histoire naturelle, Paris, France.

[2]Institut des Sciences de l'Evolution, UMR 5554, CNRS, IRD, EPHE, Université de Montpellier, Montpellier, France.

[3]Mammal Section, Life Sciences, Vertebrate Division, The Natural History Museum, Cromwell Road, London SW7 5BD, UK.

[4]Institut Pasteur de la Guyane, BP 6010, 97300 Cayenne, French Guiana.

[5]Association Kwata, BP 672, 97300 Cayenne, French Guiana.

Corresponding Author

Guillaume BILLET, guillaume.billet@mnhn.fr

Abstract

Background. With their Pan-American distribution, long-nosed armadillos (genus *Dasypus*) constitute an understudied model for Neotropical biogeography. This genus currently comprises seven recognized species, the nine-banded armadillo (*D. novemcinctus*) having the widest

distribution ranging from Northern Argentina to the South-Eastern US. With their broad diversity of habitats, nine-banded armadillos provide a useful model to explore the effects of climatic and biogeographic events on morphological diversity at a continental scale.

Methods. Based on a sample of 136 skulls of *Dasypus* spp. belonging to six species, including 112 specimens identified as *D. novemcinctus*, we studied the diversity and pattern of variation of paranasal cavities, which were reconstructed virtually using µCT-scanning or observed through bone transparency.

Results. Our qualitative analyses of paranasal sinuses and recesses successfully retrieved a taxonomic differentiation between the traditional species *D. kappleri*, *D. pilosus* and *D. novemcinctus* but failed to recover diagnostic features between the disputed and morphologically similar *D. septemcinctus* and *D. hybridus*. Most interestingly, the high variation detected in our large sample of *D. novemcinctus* showed a clear geographical patterning, with the recognition of three well-separated morphotypes: one ranging from North and Central America and parts of northern South America west of the Andes, one distributed across the Amazonian Basin and central South America, and one restricted to the Guiana Shield.

Discussion. The question as to whether these paranasal morphotypes may represent previously unrecognized species is to be evaluated through a thorough revision of the *Dasypus* species complex integrating molecular and morphological data. Remarkably, our recognition of a distinct morphotype in the Guiana Shield area is congruent with the recent discovery of a divergent mitogenomic lineage in French Guiana. The inflation of the second medialmost pair of caudal frontal sinuses constitutes an unexpected morphological diagnostic feature for this potentially distinct species. Our results demonstrate the benefits of studying overlooked internal morphological structures in supposedly cryptic species revealed by molecular data. It also

illustrates the under-exploited potential of the highly variable paranasal sinuses of armadillos for systematic studies.

Introduction

Detection of cryptic diversity and pertinent delimitation of extant taxonomic entities constitute a major challenge of current-day biological research as it may have critical implications on biodiversity conservation policies (Carstens et al., 2013). Cryptic species can be defined as "two or more species that are, or have been, classified as a single nominal species because they are at least superficially morphologically indistinguishable" (Bickford et al., 2007: 149). According to this definition, the absence of diagnostic morphological characters may have impeded the recognition of species. Depending on the case, this absence might be real (*i.e.*, populations of two cryptic species do not differ significantly in their entire anatomy) or spurious (*i.e.*, morphological differences have been overlooked).

Advanced methods of micro computed tomography (μCT) now enable an unprecedented assessment of internal anatomical structures, which can help uncover previously concealed morphological differences between taxa. The development of these non- destructive methods permits internal anatomy to be easily and systematically investigated in many taxa. These methodological improvements offer great opportunities for morphology-based phylogenetic research. In mammals, internal cranial structures certainly present a great wealth of phylogenetically informative anatomical features (e.g., Farke, 2010; Macrini, 2012; Ruf, 2014; Billet, Hautier & Lebrun, 2015), possibly as many as the external surface of the skull. There is therefore a possibility that this large proportion of previously poorly explored morphological data contains undetected morphological differences between alleged cryptic taxa.

The pan-American nine-banded armadillo (*Dasypus novemcinctus*) presents the largest distribution of any living xenarthran species (McDonough and Loughry 2013), and constitutes an interesting model for Neotropical phylogeography. Several subspecies (five to seven) have been recognized within this species but their delineation and recognition are not consensual (Cabrera, 1958; McBee and Baker, 1982; Wetzel et al., 2008; McDonough & Loughry 2013). In fact, most potential diagnostic characters for these subspecific distinctions are seldom detailed, often inconstant, or based on a limited number of observations (e.g., Peters, 1864; Allen, 1911; Lönnberg, 1913; Hamlett, 1939; Hooper, 1947; Russell, 1953). Taxonomy and phylogeny in long-nosed armadillos (Dasypodidae, sensu Gibb et al., 2016) particularly suffer from strong disagreement between morphological and molecular data (Castro et al., 2015; Gibb et al., 2016). Even though it was more focused on higher taxonomic levels, a recent study suggested the existence of an unrecognized species in French Guiana based on mitochondrial data (incl. mitogenomes) (Gibb et al., 2016). The Guianan entity has never been distinguished from other *D. novemcinctus* on a morphological basis, and might thus represent another striking case of cryptic species.

In order to explore if internal parts of the skull contain a useful phylogenetic signal, we investigated the internal paranasal sinuses and recesses (Rossie, 2006), whose complex structure has largely been ignored by morphologists working on the systematics of long-nosed armadillos (genus *Dasypus*). Based on μCT images of skulls, we reconstructed virtually the entire network of paranasal spaces in *Dasypus* species with a particular focus on specimens of *D. novemcinctus* covering the entire geographic range of the species. The observed patterns are described and discussed considering traditional taxonomic entities of long-nosed armadillos and in light of most recent molecular findings. A focus is made on the discriminatory power of these concealed

characters in armadillos and on their utility for diagnosing taxonomic units previously regarded as cryptic.

Materials & Methods

Specimens and µCT-scanning

The total number of investigated specimens is composed of 136 skulls of *Dasypus* spp. harvested from various institutions worldwide (see details in Table S1), among which 112 were identified as *D. novemcinctus,* 1 as *D. sabanicola,* 13 as *D. kappleri*, 4 as *D. hybridus*, 3 as *D. septemcinctus*, and 3 as *D. pilosus*.

Among this sample, we virtually reconstructed the internal paranasal spaces in 51 µCT-scanned specimens belonging to *D. novemcinctus* (n=47), *D. kappleri* (n=1), *D. hybridus* (n=1), *D. septemcinctus* (n=1), and *D. pilosus* (n=1). Among the 47 *D. novemcinctus* specimens, 7 were considered juveniles, including a potential stillborn (NMNH 020920); the 40 remaining being adults or subadults. Age classes (juveniles vs subadults or adults) were determined based on the stages of eruption of the teeth (Ciancio, Castro & Asher, 2012), on suture closure, and on size. The 47 *D. novemcinctus* specimens came from: United States (n=3), Mexico (n=4), Guatemala (n=1), Nicaragua (n=1), Costa Rica (n=1), Panama (n=1), Colombia (n=6), Venezuela (n=2), Ecuador (n=2), Peru (n=2), Bolivia (n=2), Paraguay (n=1), Guyana (n=3), Suriname (n=2), French Guiana (n=3), Brazil (n=12; see a list of different states in Table S1), and Uruguay (n=1). Digital data of all 51 specimens were acquired using X-ray micro computed tomography (µCT). Most specimens were scanned on the X-ray tomography imagery platform at the Université de Montpellier (France) and on the µCT-scan platform of the Imaging and Analysis Centre of the

British Museum of Natural History (London, UK); one (MNHN.ZM-MO 2001.1317) was scanned at the Museum National d'Histoire Naturelle (France) in Paris (AST-RX platform). Detailed information about the scans and acquisition parameters can be found in Table S1. Three-dimensional reconstructions and visualizations of the frontal sinuses were performed using stacks of digital µCT images with AVIZO v. 6.1.1 software (Visualization Sciences Group 2009).

An additional subset of 65 *D. novemcinctus*, 1 *D. sabanicola*, 12 *D. kappleri*, 3 *D. hybridus*, 2 *D. septemcinctus* and 2 *D. pilosus* specimens was added to the sample mentioned above. These additional specimens correspond to:

i) skulls not available for µCT-scanning but that allowed observing frontal sinuses boundaries through bone transparency through direct observations or photographs (NB: this was not possible for all observed skulls, some being insufficiently prepared or having no transparency of the frontal bone);

ii) µCT-scanned skulls whose paranasal cavities were not virtually reconstructed but their boundaries observed with ISE-Meshtools (Lebrun, 2008) with an artificial cutting of the specimen following a coronal section and with the software Landmark 3.6 (available at http://graphics.idav.ucdavis.edu/research/EvoMorph ; Institute for Data Analysis and Visualisation ©) with the option transparent surface rendering.

These two methods helped us to increase the number of investigated specimens and, most particularly, to include a paratype specimen of *D. sabanicola* (Mondolfi, 1968) (Table S1) (see discussion for a word on the status of *D. sabanicola*). In order to identify a cavity observed with

136 these alternative methods, we used similarities in position, shape, and topographical relationships
137 with sinuses or recesses defined in virtually reconstructed specimens.
138
139
140 ***Nomenclature of paranasal anatomy***
141 To our knowledge, no detailed description of paranasal cavities exists for extant armadillos,
142 except for histological slices in Reinbach (1952a & b). A maxillary recess is mentioned and
143 figured in *Euphractus* (Wible & Gaudin, 2004) and brief notes were reported on the soft
144 paranasal anatomy in *Dasypus* (Soares da Silva et al., 2016). The most extensive work on
145 paranasal spaces in Cingulata concerns in fact some glyptodonts (Fernicola et al., 2012), whose
146 sinuses are very different from that of long-nosed armadillos. For these reasons, our
147 nomenclature follows several conventions used in other taxa, as detailed below. The standard
148 practice for paranasal sinuses is to name them after the bones they excavate (Novacek, 1993); we
149 respected this practice for all the cavities we detected (i.e., both sinuses and recesses). The
150 identity of the bones housing these cavities was determined through the examination of juvenile
151 specimens that display clearly visible bone sutures. Following recent works by Maier (2000),
152 Rossie (2006), and Farke (2010), we made a distinction between sinus and recess for paranasal
153 cavities. Paranasal sinuses are pneumatic and mucosa-lined spaces that are located in the bones
154 surrounding the nasal chamber (Rossie, 2006; Curtis & Van Valkenburg, 2014). Contrary to
155 sinuses that are found between two layers of cortical bones (e.g., frontal), paranasal recesses are
156 defined as simple concavities of the nasal cavity, and are not associated with active bone removal
157 (Farke, 2010; Rossie, 2006). Hereafter, we employed the terms sinus or recess accordingly.
158 However, some cavities may apply to both definitions, with the posterior part expanding into the

bone while the anterior part only represents a concavity. In order to avoid confusion in giving two names to a single structure, we called sinuses the cavities that were at least partly comprised between two layers of a cortical bone. Because there are often several sinuses or recesses within a given bone (e.g., frontal, maxillary), we also used the English equivalents of positional terms of the Nomina Anatomica Veterinaria (NAV, 2005) for the paranasal sinuses when feasible (e.g., caudal frontal sinus). It was not possible to elaborate robust homology hypotheses for all cavities of the paranasal region because they are found in large numbers and may represent neoformations when compared to the common terminology. Consequently, we complemented the common terminology with a numbering system that allows distinguishing the numerous frontal recesses and sinuses found in long-nosed armadillos. The terminology for turbinal bones, which are only briefly mentioned for spatial localization of paranasal cavities, is based on Van Valkenburgh, Smith & Craven (2014) and Maier & Ruf (2014).

Institutional abbreviations: AMNH, American Museum of Natural History, New York, USA; BMNH, British Museum of Natural History (Natural History Museum), London, UK; IEPA Instituto de Pesquisas Científicas e Tecnológicas do Estado do Amapá in Macapá, Brazil; KWATA, Kwata Association collection, Cayenne, French Guiana; LSU, Louisiana State University, Baton Rouge, LA, USA; MBUCV Museo de biología de la Universidad central de Venezuela; MHNG, Muséum d'Histoire Naturelle in Geneva, Switzerland; MNHN.ZM.MO, collections "Zoologie et Anatomie comparée, Mammifères et Oiseaux" of Muséum National d'Histoire Naturelle, Paris, France; MUSM Museo de Historia Natural-Universidad Nacional Mayor de San Marcos, Lima, Peru; NMNH, National Museum of Natural History, Smithsonian

Institution; Washington, DC, USA; RMNH, Naturalis Biodiversity Center, Leiden, Netherlands (Rijksmuseum van Natuurlijke Historie); ROM, the Royal Ontario Museum in Toronto, Canada.

Anatomical abbreviations and measurements: CFS, caudal frontal sinus (numbered from 0 to 5); FR, frontal bone; LA, lacrimal bone; LTC, length total cranium, measured from the anterior nasal tip to the posteriormost extent of the nuchal occipital crests; NA, nasal bone; NSP, nasopharynx; RFR, rostral frontal recess (numbered from 1 to 3); RL, lacrimal recess (numbered from 1 to 2); RMXC, caudal maxillary recess; RMXR, rostral maxillary recess, ZA, zygomatic arch.

Results

Observations common to all long-nosed armadillos (genus Dasypus*)*

In all investigated long-nosed armadillos, paranasal sinuses and recesses consistently excavate the same three bones of the cranial face and vault: the lacrimal, the maxillary and the frontal. Sinuses are present only in the frontal bone of *D. novemcinctus*, *D. pilosus*, and *D. kappleri*; they are absent or weakly marked in *D. hybridus* and *D. septemcinctus* (Fig. 1). Only the posterior pneumatic parts of the frontal bone form sinuses whereas, more anteriorly, the pneumatization of the frontal bone forms recesses, which are in direct contact with the underlying turbinals all along their anteroposterior length. In most adult individuals of *D. novemcinctus* (see more details below) and *D. kappleri*, the frontal sinuses are almost entirely bordered by the posterior part of the fronto- and ethmoturbinals ventrally. In all species, the frontal sinuses and recesses regularly

increase in height toward the front. The number of sinuses and recesses varies intragenerically and these structures will be described hereafter.

In all *Dasypus* species, recesses are positioned dorsolaterally in the paranasal cavity. These recesses represent large free-of-bone spaces in the nasal cavity, generally separating turbinal bones medioventrally from the bones that build up the cranial walls. The lacrimal recesses are in contact with the mass of fronto- and ethmoturbinals medially, whereas the maxillary recesses are bordered by the naso- and maxilloturbinalsventromedially . Two distinct lacrimal recesses are invariably present and are separated by the bony cover of the nasolacrimal duct. Two recesses, variably individualized, excavate the maxillary bone (Fig. 1) and are bordered by the nasolacrimal duct ventrolaterally. These maxillary cavities may well be homologous to the maxillary sinus found in other mammals, but they are here designated as recesses following the rationale specified in the Material and Methods Section.

In addition to the taxonomic and geographic variation described below, variable levels of intra-individual asymmetry appear to affect all species and all paired paranasal spaces under consideration here. This asymmetry is not directional, it is ubiquitous and present in most if not all specimens, which suggests a case of fluctuating asymmetry (Van Valen, 1962). The species *D. kappleri* seems to be characterized by stronger levels of asymmetry than the species *D. novemcinctus* (see below).

***Juveniles of* D. novemcinctus**

In addition to delivering critical information on the identity of bones housing the various sinuses and recesses, the study of juvenile individuals provided some clues on the growth pattern of the paranasal pneumatization in the nine-banded armadillo. Juveniles show a less tight medial

contact between paired medial sinuses, such as the rostral frontal recesses (which may split in RFR1 and RFR1', see below) or the caudal frontal sinuses (Fig. 2). Compared to adults, caudal frontal sinuses (CFS) are less expanded posteriorly in juveniles and do not lie above the most posterior part of the mass of fronto- and ethmoturbinals.

A very young specimen (likely a stillborn, AMNH 33150) shows that very early ontogenetic phases of paranasal pneumatization start with a weak individualisation of the caudal maxillary recess, whereas no other sinus or recess is individualized and the turbinals are not yet ossified. The large cavity excavated in the posterior part of the frontals in this specimen does not represent a sinus but a transverse canal, presumably for the frontal diploic vein (Wible and Gaudin, 2004) (Fig. 3). Other juveniles in our dataset clearly correspond to later ontogenetic stages, as indicated by their size: LTC= AMNH33150 38,93mm; LSU3244 66,14mm; NMNH 020920 72,89mm; AMNH133259 68,85mm (NB: LTC ~ 90-105mm in adults; Hautier L., unpublished data). This age difference is confirmed by their stage of dental eruption: first decidual bicuspid tooth erupting in AMNH 33150; dP1-dP7 present in LSU3244 and NMNH 20920; dP1-dP7 and alveolus of M1 present in AMNH 133259 (see Ciancio et al., 2011). The juvenile series shows that paranasal pneumatization and turbinal ossification just barely started in perinatal stages lesser than 40% adult skull length (AMNH 33150; Fig. 3) whereas these structures are well-developed in later stages with dp1-dp7 erupted and with ~70% of adult skull length (Fig. 2).

Observations common to all adults of nine-banded armadillos (*D. novemcinctus*)

Skulls of adult *D. novemcinctus* are more pneumatized than juvenile ones (Figs. 2-4). All adult *D. novemcinctus* present a similar pattern of sinuses: posteriorly, a number of 5 to 6 paired CFS

generally cover dorsally the posterior part of the mass of fronto- and ethmoturbinals (Figs. 1, 4 and 5). One medialmost and often reduced pair of CFS was identified as variably present and designated as CFS 0, in order to start numbering from 1 for the invariably present CFS. The set of CFS form a continuous transversal chain of dorsal paranasal spaces between the orbits (Fig. 5). While the posterior part of each CFS is comprised between two layers of cortical bone, the anterior part is always bordered ventrally by the fronto- and ethmoturbinals (Fig. 5). Anterior to the CFS, the frontal bone houses several pairs of rostral frontal recesses (RFR). These recesses show variable shapes (see below), but can be at least divided in two main areas: a medial recess generally elongated (RFR1) and/or subdivided anteroposteriorly (RFR1 & RFR1'), and a recess or group of recesses that excavate the frontal bone more laterally up to the lacrimal recesses (RFR2-3) (Fig. 1). Topographical criterions were used for establishing homologies and numbering of the CFS, with the CFS 0-1 always located directly posterior to the RFR1 and the CFS2-4 located posterior to the RFR2-3. In our sample of *D. novemcinctus*, the RFR1 are always bordered posteriorly by one or two pairs of CFS in our sample of *Dasypus novemcinctus*. When two pairs are present, the medialmost (or anteriormost in a few specimens; see below), CFS 0, is always the smallest. Therefore, we consider that the medialmost pair is CFS1 when only one pair is present (Figs. 1 and 4).

***Northern morphotype of* D. novemcinctus**

Thirty nine (39) specimens from North and Central America and from the Pacific coast of eastern Ecuador are attributed to this morphotype (Figs. 1, 4 and 6). Specimens attributed to this group originate from (in alphabetical order of countries): Belize, Colombia (Antioquia Department), Costa Rica, Ecuador (Provinces El Oro and Pichincha), Guatemala, Honduras,

Mexico (Sinaloa, Tabasco, Oaxaca, Colima, Jalisco, and an undetermined locality (NMNH179172) for the adults, San Luis Potosi and Morelos for the juveniles), Nicaragua, and USA (states of Mississipi, Texas, Florida, Kansas, and Louisiana). The main diagnostic feature for this group is the anteroposterior elongation of the CFS2 to 5; in addition, the left and right CFS2 are obliquely orientated and contact each other posterior to the CFS1. Another distinctive feature of this morphotype is the subdivision and the relative shortening of RFR1. As for the Southern morphotype (see below), the number of CFS pairs in this group varies from 5 to 6, because the CFS0 pair is either very reduced or absent. The CFS1 are rather small, shorter than the more lateral CFSs and bordered posteriorly by the contacting pair of CFS2. The CFS2 and/or CFS3 are the largest CFSs within this group, and though they do not contact posteromedially, each CFS3, similarly to the CFS2, bends or orientates obliquely toward the midline posteriorly. The CFS4 can be as elongated as the CFS2-3 or slightly smaller; the CFS5 are more reduced. The median rostral frontal recesses are subdivided into two anteroposterior pairs RFR1 and RFR1' and contrast with the long RFR1 of the Southern morphotype. The posterior pair, the RFR1, apparently forms earlier within the ontogenetic sequence as it is clearly more developed than RFR1' in two juvenile specimens from Mexico (Fig. 2). The shape of RFR1 in adults is rather square whereas the anterior pair, RFR1', is usually slightly more elongated anteroposteriorly. Lateral to the RFR1 and RFR1', the RFR2 and 3 are often well separated (distinction often better marked than in the Southern group); the RFR3 is immediately lateral to the RFR2. The same applies to the caudal and rostral maxillary recesses (RMXC & RMXR), which are often better separated in this morphotype compared to the Southern morphotype; the caudal maxillary recess is posterolateral to the rostral one and located just anterior to the lacrimal recess 2.

295 The specimen AMNH 40984 from southwest Ecuador is attributed to this Northern group
296 because of the presence of large and posteriorly convergent CFS2 and short and subdivided
297 RFR1-RFR1' (Fig. 4). The other specimen from western Ecuador, BMNH 16.7.12.37, also
298 shows these characters through bone transparency. Nevertheless, on the virtual reconstruction of
299 AMNH 40984, the lateral RFR2-3 appear more subdivided than in other members of this
300 morphotype, and also more than in other morphotypes. In addition, the anterior edge of its
301 medialmost CFS (CFS 0) is shifted anteriorly. These unique characters could not be checked on
302 the specimen observed on photos only.
303
304 ***Southern morphotype of*** **D. novemcinctus**
305 Fifty one (51) specimens (incl. the paratype of *D. sabanicola*) spanning the Amazon Basin
306 (excluding the Guiana Shield) and including the southernmost distribution of the species in
307 Uruguay show a distinct pattern of paranasal spaces (Figs. 4 and 6). Specimens attributed to this
308 group thus span the Southern range of *D. novemcinctus* and originate from the following
309 countries (in alphabetical order): Bolivia (states of Beni, Pando and Santa Cruz), Brazil (states of
310 Amazonas, Para, Goias, Santa Catarina, Mato Grosso, Mato Grosso do Sul, Minas Gerais, São
311 Paulo, Rio Grande do Sul and Espirito Santo), Colombia (Meta and Magdalena departments),
312 Ecuador (Morona Santiago Province), Paraguay, Peru (regions of Ucayali, Ayacucho and San
313 Martín), Uruguay, and Venezuela (states of Anzoátegui and Apure (state of the paratype of *D.*
314 *sabanicola*)). The distinctive features of the Southern pattern of paranasal spaces mostly consist
315 in an anteroposteriorly reduced posterior chain of caudal frontal sinuses and an elongated rostral
316 frontal recess 1 (Figs. 1 and 4). In this group, the CFS0 are variably present. When present, they
317 are generally smaller than the more lateral CFS1 to 5. The CFS1 always contact each other

318 medially, or just at their posteromedial corner if the CFS0 are present. In most specimens, the
319 CFS are much shorter anteroposteriorly than the rostral frontal recess RFR1, usually around a 1/2
320 or 1/3 ratio. Some specimens referred to this morphotype show more balanced ratios but the
321 anteroposterior length of the CFS never exceeds that of the RFR1. The CFS1 to 4 are usually of
322 similar length and width, the areas of the CFS 1 and 2 may just slightly exceed that of the others
323 in average. The lateralmost caudal frontal sinus that lies immediately medial to the orbital rim,
324 i.e. the CFS5, is generally shorter than the other CFS.

325 Additionally, many individuals of that group show a weak distinction or even a fusion
326 between the RFR2 and 3 (Figs. 1 and 4). Though the RFR2 and 3 are in average less separated
327 than in other groups of *D. novemcinctus*, this character is not stable within the Southern group.
328 Ontogenetic data are unfortunately lacking to state on a possible influence of development on
329 this feature. When not completely fused, the RFR 2 and 3 are often separated by a short bony
330 ridge posteriorly.

331 The maxillary recesses are located dorsal to the nasolacrimal duct and (antero)lateral to
332 the RFR1. As for the RFR2 and 3, the caudal and rostral maxillary recesses are variably distinct;
333 in average, they are less separated than in the other groups.

334

335 ***Guianan morphotype of* D. novemcinctus**

336 Seventeen (17) specimens are attributed to this group and originate from: Brazil (Amapa State),
337 French Guiana, Guyana and Suriname. The most conspicuous diagnostic feature of this group is
338 the strong inflation of the CFS2, which is by far the largest caudal frontal sinus (Figs. 1, 4, 5 and
339 6). These hypertrophied CFS2 occupy most or all the pneumatized frontal area between the
340 orbits up to the level of the anterior edge of the posterior zygomatic root posteriorly. More

341 precisely, it is the posterior part of the CFS2 that is hypertrophied and borders all or most other
342 CFSs on their caudal side. The anterior part of the CFS2, which is sandwiched between CFS1
343 and CF3, is as narrow as the CFS3-4. The outline of CFS2 often exhibits a complex irregular
344 pattern and pairs are clearly asymmetric in all specimens (Fig. 4).

345 The CFS0 are variably present as in other groups. When present, they are rather small,
346 clearly elongated transversally and entirely bordered by the CFS1 posteriorly. In comparison to
347 other morphotypes, the CFS0 are slightly shifted anteriorly relative to other CFSs. The size and
348 shape of the CFS1 is also variable. In specimens with no CFS0, the CFS1 are much reduced and
349 rather square-shaped (AP 207; Fig. 4). In specimens with CFS0, the CFS1 are relatively larger
350 and can extend as far posteriorly as the hypertrophied CFS2. In such case (MNHN.ZM-MO
351 2001-1317), they are transversally thin and sandwiched between the pairs of CFS2 (Fig. 4). In
352 one specimen (MNHN.ZM-MO 1996-587), the CFS1 seems to be partly fused posteromedially
353 with the CFS2 on both sides. The CFS3 and 4 are considerably smaller than the CFS2, and are
354 similar in size as in the Southern morphotype. The CFS5 is generally smaller than CFS3-4, and
355 can be absent (*e.g.*, MNHN.ZM-MO 2001-1317).

356 The configuration of the RFR1 is variable, as they seem to be irregularly divided into an
357 anterior RFR1' and posterior RFR1. The limits between these two subdivisions are not only
358 variable between individuals of this morphotype, they are also labile intra-individually: the
359 subdivisions may be marked on one side of the skull, not on the other (ROM 32275) or it may
360 follow another path (MNHN.ZM-MO 1995-553), or the boundaries may be irregularly marked
361 overall (marked on some portion, then absent, and then marked again a little farther away;
362 NMNH 339668). As in the Southern morphotype, the RFR2 and 3 are poorly distinguishable in

363 most Guianan specimens (but this is also variable), except for a posterior demarcation that is
364 almost always present.
365 The lacrimal recesses 1 and 2 are very similar to that of the other morphotypes, also
366 delimited by the nasolacrimal duct. The intensity of the separation between the rostral and caudal
367 maxillary recesses is variable, but these recesses are otherwise very similar to other
368 morphotypes.
369
370 ***Problematic Specimens from Panama, Venezuela and Colombia***
371 Five specimens (AMNH 32356, 37356, NMNH 281290 from Colombia, BMNH 5-7-521 from
372 Merida, Venezuela and NMNH 171052 from Panama) show somewhat intermediate
373 morphologies between the Southern and Northern morphotypes (Fig. 4). They all present CFS
374 and RFR1 of similar length and do not show a medially contacting pair of CFS2 (though close in
375 AMNH 37356). The RFR1 are usually not subdivided, except in the Venezuelan specimen and,
376 to a lesser extent, in the Colombian AMNH 32356. The CFS2 and 3 do not represent the largest
377 CFS except in the Colombian AMNH 32356 and 37356. These specimens therefore show a
378 combination of features characterizing the Southern and Northern groups.
379 In addition, the probable stillborn specimen AMNH 33150 from Colombia could not be referred
380 to any morphotype because its paranasal spaces are not fully developed yet (Fig. 3).
381
382 ***Other* Dasypus *Species***
383 *Greater long-nosed armadillo (*D. kappleri*)*
384 The *D. kappleri* specimens present a large pneumatization of their paranasal region, as in *D.*
385 *novemcinctus*. However, all *D. kappleri* specimens exhibit less numerous, but wider and longer

finger-shaped CFS than *D. novemcinctus*. In fact, this may be due to various partial or complete fusions of the CFS with the RFR, which we tentatively identify as follows: the CFS1 and RFR1 are fused and occupy the medialmost region (but not posteriorly in some specimens; see below), the CFS2-3 are fused with the RFR2-3 (Fig. 1). We consider that the caudal end of these structures are homologous to the CFS since it is found between two layers of frontal bone. In some specimens, a blunt bony bridge still marks a separation between these sinuses and recesses. This general pattern is typical of the species, yet the arrangement of paranasal cavities largely varies intraspecifically. Two groups can be distinguished: specimens from the Guiana Shield display fused CFS1-RFR1 that reach the posterior boundary of the other CFS, whereas specimens from more western locations have the right and left CFS2 that contact posteriorly in the midline (Fig. S1). The relative sizes of the CFS also vary a lot, but the fused CFS2-3 with RFR2-3 are in most cases the largest ones. In addition, most of these recesses show a substantial amount of asymmetry, probably higher than in *D. novemcinctus*. Other recesses are grossly similar in size and location to those described for *D. novemcinctus*.

*Hairy long-nosed armadillo (*D. pilosus*)*

The investigated specimens of *D. pilosus* probably resemble the most the *D. novemcinctus* groups (Fig. 1). Conversely to *D. kappleri*, specimens of *D. pilosus* show caudal frontal sinuses well-individualized from the rostral frontal recesses. However, there is some variation in the shape of the caudal frontal sinuses. In the only scanned specimen of *D. pilosus*, the caudal frontal sinuses are barely recognizable as they do not excavate the frontal bone (not found between two layers of frontal bone); they are located just dorsal to the mass of fronto- and ethmoturbinals. In fact, they rather represent thin cell-shaped recesses with irregular outlines, which are sandwiched

409 between the frontal bone dorsally and the fronto- and ethmoturbinals ventrally. Conversely, the
410 two additional specimens of *D. pilosus* observed through bone transparency show slightly longer
411 caudal frontal sinuses/recesses that are better delineated. In any case, these caudal cell-shaped
412 frontal sinuses/recesses are in all three specimens comparable to the CFS of *D. novemcinctus*
413 groups in their number (4 to 5 pairs), dorsal outline and location. The rather short anteroposterior
414 extent and reduced mediolateral width of these CFS-like structures in *D. pilosus* are most
415 reminiscent of the pattern seen in the Southern group of *D. novemcinctus*. The more anterior
416 recesses resemble the RFR1 and RFR2-3 of the same Southern group, especially the
417 un(sub)divided and elongated RFR1. Remarkably, the lacrimal recesses are more elongated
418 anteroposteriorly than in other *Dasypus* species.
419
420 *Southern long-nosed armadillo (*D. hybridus*) and seven banded armadillo* (D. septemcinctus*)*
421 These two species are here described together because they exhibit strong similarities in their
422 pattern of paranasal cavities and could not be distinguished in our sample. These two small-sized
423 species show the least pneumatized skulls among our adult sample of *Dasypus*. Both species
424 present RFR1 that are transversely narrow and curved, never in contact medially, and thus partly
425 recall the configuration seen in young *D. novemcinctus* specimens (see above) (Figs. 1-2). In
426 addition, specimens of both species have poorly defined CFS, i.e., the fronto- and
427 ethmoturbinals fill in most of the space just ventral to the cranial vault made by the frontals and
428 the CFS are very thin dorsoventrally. The frontal bones are in fact poorly pneumatized and show
429 a thin diploe. Other cavities (rostral frontal recesses, lacrimal and maxillary recesses) show a
430 pattern and extent grossly similar to that of other *Dasypus* species.
431

Discussion

Distribution and significance of paranasal pneumatization in mammals and armadillos

Paulli (1900a; 1900b) first provided detailed descriptions of paranasal cavities based on sagittal and transverse osteological sections of mammalian skulls. With the recent development of μCT and virtual modeling of internal structures, the paranasal sinuses and recesses could be more systematically and precisely studied in extant mammals such as vombatiform marsupials, carnivorans, artiodactyls, and primates (e.g., Rossie, 2008; Farke, 2010; Curtis & Van Valkenburg, 2014; Maier & Ruf, 2014; Sharp, 2016). Though not yet thoroughly investigated with modern techniques, these structures are also known to occur in many other groups of placental mammals (Paulli, 1900a; Paulli, 1900b; Edinger, 1950; Novacek 1993) and may constitute convergently lost symplesiomorphic placental features (Foster & Shapiro, 2016).

The ubiquitous distribution of these structures in several clades of amniotes (Witmer, 1999) long raised questions regarding the potential functional role of paranasal pneumatization. As noted by Farke (2010: 988), cranial pneumatization such as paranasal sinuses "remains one of the most functionally enigmatic and debated structures within the vertebrate skull". Indeed, researchers have long speculated on the potential functional role of these air-filled chambers, and proposed a wealth of hypotheses (Blanton & Biggs, 1969; Blaney, 1990; Marquez, 2008), most of which remain, as of today, untested. However, one of the current dominating hypotheses regards sinuses as functionless structures influenced by constraints inherent to bone growth and patterning (Witmer, 1997; Smith et al., 2005; Farke, 2010 and citations therein). In fact, sinuses may just opportunistically fill space where bone is not mechanically necessary (Curtis & Van Valkenburg, 2014) and reduce skull mass in return (Curtis et al., 2015). This might be compatible with the fact that the presence and extent of sinuses may, at least in some instances,

455 be linked to size increase and to the shape of the bone in which they are contained (Weidenreich,
456 1941; Zollikofer et al., 2008; Farke, 2010; Curtis et al., 2015; Krentzel & Angielczyk, 2016; Ito
457 & Nishimura, 2016; Sharp & Rich, 2016). Though these alternative architectural explanations do
458 not preclude the existence of functional advantages (e.g., to dissipate mechanical stress during
459 biting; Tanner et al., 2008), it seems that there is no overarching explanation for the function of
460 sinuses (Curtis et al., 2015).

461 A substantial variation of paranasal sinuses shape and outline has long been noted in
462 many taxa at the interspecific, intraspecific, and intra-individual levels (e.g., Paulli, 1900a;
463 Paulli, 1900b; Novacek, 1993; Farke, 2010; Curtis & Van Valkenburg, 2014). These
464 observations clearly suggest that these structures have a non-negligible propensity to vary greatly
465 in mammals. It is questionable whether or not their high variability (sensu Hallgrímsson & Hall,
466 2005) could make paranasal sinuses good markers of phylogenetic history. Interestingly, the
467 highly variable shape and size of the frontal sinus in modern humans proved to be largely
468 inherited from parents to children (Szilvássy, 1982) and is used in forensic science for individual
469 and population identifications (e.g., Kim et al., 2013). At higher taxonomic levels, a significant
470 phylogenetic signal was detected in the pattern of paranasal sinuses of primates and bovid
471 artiodactyls (Rossie, 2008; Farke, 2010), but the size and shape of frontal sinuses were rather
472 weakly linked with phylogenetic groupings in Carnivora (Curtis & Van Valkenburg, 2014).
473 Similarly, the diversity of maxillary sinuses in macaques was not linked to phylogeny (Ito &
474 Nishimura 2016) even though these structures were at least in part controlled by intrinsic genetic
475 factors (Ito et al., 2015).

476 In the case of long-nosed armadillos, the clear discrete differences in patterns of paranasal
477 sinuses observed between the different species and subgroups of *Dasypus* (*D. novemcinctus*, *D.*

478 *kappleri*, *D. pilosus*, *D. septemcinctus* and *D. hybridus*) argue for a high discriminatory power
479 and a good phylogenetic signal carried by these structures within the genus. The fluctuating
480 asymmetry (Van Valen, 1962) tentatively identified for these structures in armadillos suggests
481 that they are also impacted by random perturbations of developmental processes (Klingenberg,
482 2010). Curiously, early anatomical accounts of paranasal anatomy disagreed on the presence of
483 sinuses in long-nosed armadillos. While Cuvier (1845) and Weinert (1925) correctly observed
484 the presence of such structures in long-nosed armadillos, other early authors overlooked it
485 (Paulli, 1900b; Zuckerkandl, 1887 (as cited in Weinert, 1925)). In fact, frontal sinuses were still
486 considered absent in armadillos as a whole in recent anatomical works (Novacek, 1993). Our
487 results clearly contradict these considerations and investigation of paranasal cavities in some
488 Chlamyphoridae, the sister group of Dasypodidae within Cingulata (Gibb et al., 2016), even
489 reveals homoplastic evolution of these structures in armadillos. Frontal sinus or recesses are
490 absent in the extant chlamyphorid *Euphractus sexcinctus* (Wible & Gaudin, 2004) and some
491 µCT-scanned specimens of *Cabassous unicinctus* (MNHN.ZM.MO 1953-457) and *Zaedyus*
492 *pichiy* (MNHN.ZM.MO 1917-135) do not show any free-of-bone space between the frontal and
493 the fronto- and ethmoturbinals (personal observations). On the other hand, an extensive system
494 of paranasal sinuses exists in the extinct glyptodont *Neosclerocalyptus* (Fernicola et al., 2012).
495 Further comparisons are needed in extant and fossil forms (see sinuses in the fossil *D. punctatus*,
496 Castro et al., 2013), as these structures might provide potentially interesting characters for the
497 understanding of higher-level relationships within the order (Delsuc et al., 2016).
498
499 ***Relevance of paranasal sinuses for the systematics of long-nosed armadillos***

Our detailed investigation of paranasal cavities in *Dasypus* species revealed an important variation at different levels. We briefly described the ontogenetic pattern of the paranasal sinuses and recesses, which may start individualizing in perinatal stages (see also Reinbach, 1952a & b). Postnatal juvenile specimens show CFS that are less developed posteriorly when compared to adult specimens, revealing the late posterior growth of these structures. Second, as indicated above, adults show clear differences between traditionally recognized species, mostly in the configuration of the CFS and RFR. Besides the large variation seen within *D. novemcinctus* (see below), clear differences can be observed between *D. kappleri*, *D. pilosus* and the sister species *D. hybridus* - *D. septemcinctus*. The greater long-nosed armadillo (*D. kappleri*) probably has the most divergent morphology regarding these sinuses and recesses with the fusion of its CFS and RFR. In contrast, these structures are better separated in all other long-nosed armadillos reconstructed here. This is congruent with the early diverging position of *D. kappleri* in the phylogeny of long-nosed armadillos (Gibb et al., 2016). Our sample for *D. kappleri* is also characterized by a substantial variation, which is partly structured geographically: specimens from the Guiana Shield show a CFS1-RFR1 that reaches the posterior level of other CFS, whereas this is not the case in other specimens originating from more western areas in South America (Fig. S1). Interestingly, these two allopatric groupings are congruent with the new taxonomic subdivision proposed by Feijo & Cordeiro-Estrela (2016), with a revised *D. kappleri* species restricted to the Guiana Shield area, and a new species (*D. pastasae*) found from the eastern Andes of Peru, Ecuador, Colombia, and Venezuela south of the Orinoco River into the western Brazilian Amazon Basin. These preliminary results now require a larger sample, including specimens referred to *D. beniensis* (Feijo & Cordeiro-Estrela, 2016), in order to further test species delimitation in the *D. kappleri* complex.

523 The pattern of paranasal cavities of the hairy long-nosed armadillo (*D. pilosus*) is more
524 similar to the Southern morphotype of *D. novemcinctus* than to any other morphotype, which
525 may have important implications on the reconstruction of its phylogenetic affinities. Castro et al.
526 (2015) found this species to be the sister group of all other species attributed to the genus
527 *Dasypus*, and therefore proposed to place it in its own genus *Cryptophractus*. This early
528 diverging position and generic status is in disagreement with a more recent mitogenomic
529 analysis, which retrieved *D. pilosus* in a more nested position within the genus *Dasypus*, with *D.*
530 *kappleri* representing the earliest diverging species (Gibb et al., 2016). Remarkably, our findings
531 may provide new morphological arguments for such a nested position of *D. pilosus* as
532 unambiguously supported by molecular data. The related species *D. septemcinctus* and *D.*
533 *hybridus*, for their part, closely resemble each other, as it could have been expected given their
534 overall morphological resemblance and their phylogenetic proximity. This observation adds to
535 the growing body of evidence that these two parapatric species might in fact represent a single
536 taxonomic entity with a large distribution (Abba & Superina, 2010; Gibb et al., 2016).
537 Most importantly, the variation within the nine-banded armadillo (*Dasypus*
538 *novemcinctus*) allowed clearly separating three distinct geographical groups based on the pattern
539 of paranasal cavities (Fig. 6). These individual subsets do not exactly correspond to traditional
540 subspecies proposed for the nine-banded armadillo (McBee & Baker, 1982) though the
541 distinction between the Northern and Central American (Northern morphotype) and the Southern
542 American (Southern morphotype) groups may recall some subspecific boundaries (see below). In
543 fact, although bone transparency often offers the possibility to observe the boundaries between
544 the frontal sinuses and recesses, it seems that these characters have long been overlooked in
545 cingulate systematics. The most interesting result lies in the distinction of a well-characterized

546 entity restricted to the Guiana Shield area. Guianan nine-banded armadillos are distinguished by
547 an inflated CFS2 in comparison to all other armadillos investigated here. The irregular outline of
548 the CFS2 varies greatly among individuals belonging to the Guianan morphotype but its large
549 size relative to other CFS appears distinctive. While nine-banded armadillos from the Guiana
550 Shield have never been distinguished as a subspecies (i.e. they were until now considered as part
551 of the subspecies *D. novemcinctus novemcintus* Linnaeus 1758; Wetzel et al., 2008),
552 mitochondrial data showed that populations from French Guiana may represent an early
553 diverging and previously unrecognized lineage clearly separated from other *D. novemcinctus*
554 (Gibb et al., 2016). Specimens from French Guiana present unexpectedly distant mitochondrial
555 D-loop region (Huchon et al., 1999) and divergent mitogenomes (Gibb et al., 2016) from the
556 invasive US populations of nine-banded armadillos. Based on these new data, nine-banded
557 armadillos from French Guiana are supposed to have diverged 3.7 Ma ago from a clade formed
558 by other *D. novemcinctus*, *D. sabanicola*, *D. mazzai* and *D. pilosus* (Gibb et al., 2016). In this
559 regard, the new data on paranasal cavities deliver unprecedented and very enlightening results:
560 there exists a discrete morphological signal of internal cranial structures that supports the
561 distinctness not only of French Guianan specimens, but also of specimens from Suriname,
562 Guyana and the state Amapa in Brazil (Fig. 6). Based on this distribution, we refer to this entity
563 as specimens from the Guiana Shield (or Guianan specimens) whereas we do not know the exact
564 outline and boundaries of the range occupied by these distinctive armadillos. Taken together with
565 recent mitogenomic data (Gibb et al., 2016) and analyses of cranial shape variation (Hautier L.,
566 unpublished data), the paranasal autapomorphies found in this study make a strong case for the
567 distinction of nine-banded armadillo specimens from the Guiana Shield as a potentially new
568 species. The discovery of discrete paranasal characters supporting this purportedly distinct

569 species demonstrates the necessity to study internal anatomy for a truly integrative taxonomy.
570 The number and delimitation of subspecies recognized within *D. novemcinctus* has long been a
571 matter of debate among armadillo taxonomists (Cabrera, 1958; McBee & Baker, 1982; McBee,
572 1999; Wetzel et al., 2008; McDonough & Loughry 2013). Alongside the Guianan morphotype,
573 the study of paranasal cavities also permitted to distinguish a mostly North and Central American
574 morphotype (Northern group) and another South American morphotype (Southern group), which
575 largely comes from the Amazon area (Fig. 6). The Northern morphotype is characterized by i) an
576 anteroposterior elongation of the CFS2 to 5, with the obliquely oriented pair of CFS2 contacting
577 each other posteromedially, and ii) subdivided and relatively shortened RFR1. The area where
578 this morphotype is found fully covers the proposed repartition of the subspecies *D. novemcinctus*
579 *mexicanus* (Peters, 1864), *D. novemcinctus davisi* Russel 1953, and part of *D. novemcinctus*
580 *fenestratus* Peters 1864, and *D. novemcinctus aequatorialis* Lönnberg 1913 (McBee & Baker,
581 1982; Wetzel et al., 2008; McDonough & Loughry, 2013). It is generally well distinguished from
582 the Southern morphotype, which is characterized by an anteroposteriorly reduced posterior chain
583 of CFS and an elongated RFR1 (Fig. 6). The area occupied by specimens belonging to this
584 morphotype corresponds mostly to the subspecies *D. novemcinctus novemcintus* (to the notable
585 exception of the Guiana Shield area) and may also cover the distribution of *D. novemcinctus*
586 *mexianae* Hagmann 1908 (Wetzel et al., 2008).
587 Problematic specimens whose pattern of paranasal sinuses is not easily referable to one of
588 the three main morphotypes are present in Panama and in the eastern parts of Colombia and
589 Venezuela (Fig. 6). This geographic area also partly corresponds to the subspecies *D.*
590 *novemcinctus fenestratus* (Wetzel et al., 2008). The partial incongruence of these internal data
591 with recognized subspecies of *D. novemcinctus* raises important taxonomic issues. In addition,

592 these challenging results may also call into question the validity of the debated species *Dasypus*
593 *sabanicola* (Mondolfi, 1968; Abba & Superina, 2010; Gibb et al., 2016), whose paratype
594 MBUCV 439 exhibits the pattern of paranasal cavities of the *D. novemcinctus* Southern
595 morphotype. However, this paratype represents a subadult specimen (Mondolfi, 1968), which
596 casts doubts on the growth stage exhibited by its paranasal cavities (NB: other specimens
597 attributed to this species could not be checked). The possibility also exists that this morphotype
598 represents a plesiomorphic condition within the genus, since *D. pilosus* also exhibits a similar
599 pattern. The question as to whether or not the three *D. novemcinctus* paranasal morphotypes
600 represent natural taxonomic entities is now to be evaluated through a thorough revision of the
601 *Dasypus* species complex that should integrate various morphological aspects and substantial
602 molecular data (Hautier L., unpublished data; Arteaga M-C., unpublished data). The case of the
603 problematic specimens found in Colombia, Venezuela and Panama clearly illustrates this
604 necessity.

605 The existence of different morphotypes within the large geographical range of *D.*
606 *novemcinctus* also raises the possibility that divergent paranasal morphologies reflect adaptation
607 to different local climatic and environmental conditions. Yet, the potential functional benefits for
608 selecting one of these paranasal patterns remain obscure. Though we cannot discard that these
609 structures have different functions and architectural constraints, genetic drift might have also
610 played an important role in the differentiation of these labile structures. Geographical and
611 environmental barriers, the Andes in particular, seem to separate some of these cranial
612 morphotypes (see also Hautier et al., unpublished data), a pattern that emphasizes the role played
613 by the Andean uplift in the diversification of several xenarthrans species (Moraes-Barros and
614 Arteaga, 2015).

615

616

617 Conclusions

618 As an early worker on *Dasypus* systematics, Hamlett (1939: 335) noted that in spite of the
619 dispersion of *D. novemcinctus* through many geographical regions, "it remains so uniform that it
620 is apparently impossible to find external variations sufficiently constant to be of subspecific
621 rank". In fact, he suspected that cranial characters could offer the only promise for subspecific
622 analysis of the species. These words resonate particularly, as the strong geographical imprint
623 found in the variation pattern of paranasal cavities sheds new light on the delimitation of *D.*
624 *novemcinctus* and its subspecies. As demonstrated in this work, the investigation of frontal
625 sinuses may help to uncover previously overlooked phylogenetic subsets within the large
626 geographic range of nine-banded armadillos. This study highlights the under-exploited potential
627 of internal characters for systematic studies and their utility for detecting otherwise potentially
628 cryptic species. The strong variation and high discriminatory power found in the paranasal
629 sinuses of armadillos is even strangely reminiscent of the extremely variable frontal sinuses of
630 modern humans which can be used as forensic fingerprints (Kim et al., 2013) and kinship
631 markers (Szilvássy, 1982; Slavec, 2005). In addition to its great potential for extant species, the
632 study of the paranasal spaces also constitutes a promising approach to provide new informative
633 characters for the phylogenetic placement of fossil species of the genus *Dasypus* (e.g., see partly
634 exposed frontal sinuses in *D. punctatus*; Castro et al., 2013).

635

636 Acknowledgements

637 We are grateful to Géraldine Véron and Aurélie Verguin (Muséum National d'Histoire Naturelle,
638 Paris), Roberto Portela Miguez, Louise Tomsett, Laura Balcells and Paula Jenkins (British
639 Museum of Natural History, London), François Catzeflis and Suzanne Jiquel (Institut des
640 Sciences de l'Evolution, Montpellier), Victor Pacheco (Dpto de Mastozoología, Museo de
641 Historia Natural, Universidad San Marcos, Lima), Eileen Westwig (American Museum of
642 Natural History, New-York), Burton Lim (Royal Ontario Museum, Toronto), Edmison Nicole
643 and Chris Helgen (National Museum of Natural History, Washington), Jake Esselstyn (Louisiana
644 State University, Bâton-Rouge), Manuel Ruedi (Muséum d'Histoire naturelle, Geneva), Claudia
645 Regina da Silva (Instituto de Pesquisas Científicas e Tecnológicas do Estado do Amapá,
646 Macapá), Steven van der Mije (Naturalis Biodiversity Center, Leiden), Lucile Dudoignon
647 (KWATA association), Maria-Clara Arteaga, Maria Nazareth da Silva (Manaus Museum) and
648 their collaborators for access to comparative material. R. Lebrun (Institut des Sciences de
649 l'Evolution, Montpellier), Farah Ahmed (British Museum of Natural History, London), Miguel
650 García-Sanz (Platform AST-RX MNHN) generously provided help and advice on the acquisition
651 of µCT scans. Thanks to Sandrine Ladevèze for providing µCT-scan data for *Cabassous* and
652 *Zaedyus*. Many thanks to Alana Sharp, Irina Ruf and an anonymous reviewer for their fruitful
653 comments on this manuscript. In compliance with Advantages and Benefits Sharing policy in
654 French Guiana, material from French Guiana has been registred in the collection JAGUARS
655 (http://kwata.net/la-collection-jaguars-pour-l-etude- de-la-biodiversite.html ; CITES reference:
656 FR973A) supported by Kwata NGO, Institut Pasteur de la Guyane, DEAL Guyane, and
657 Collectivité Territoriale de la Guyane. This is contribution ISEM 2017-XXX of the Institut des
658 Sciences de l'Evolution.
659

660 ## References

661 Abba AM, Superina M. 2010. The 2009/2010 armadillo Red List assessment. *Edentata* 11:135–
662 184.

663

664 Allen GM. 1911. Mammals of the West Indies. *Bulletin of the Museum of Comparative Zoology*
665 54:175-263.

666

667 Bickford D, Lohman DJ, Sodhi NS, Ng PK, Meier R, Winker K, Ingram KK, Das I. 2007.
668 Cryptic species as a window on diversity and conservation. *Trends in Ecology & Evolution* 22
669 (3):148-155.

670

671 Billet G, Hautier L, Lebrun R. 2015. Morphological diversity of the bony labyrinth (inner ear) in
672 extant xenarthrans and its relation to phylogeny. *Journal of Mammalogy* 96(4):658–672.

673

674 Blaney SPA. 1990. Why paranasal sinuses? *Journal of Laryngology and Otology* 104:690–693.

675

676 Blanton PL, Biggs NL. 1968. Eighteen hundred years of controversy: the paranasal sinuses.
677 *American Journal of Anatomy* 124:135–147.

678

679 Cabrera A. 1958. Catalogo de los mamíferos de América del Sur. *Revista del Museo Argentino*
680 *de Ciencias Naturales "Bernardino Rivadavia," Buenos Aires* 4:1-307.

681

682 Carstens BC, Pelletier TA, Reid NM, Satler JD. 2013. How to fail at species delimitation.
683 *Molecular Ecology* 22(17):4369-4383.
684
685 Castro MC, Ciancio MR, Pacheco V, Salas-Gismondi RM, Bostelmann JE, Carlini AA. 2015.
686 Reassessment of the hairy long-nosed armadillo "*Dasypus" pilosus* (Xenarthra, Dasypodidae)
687 and revalidation of the genus *Cryptophractus* Fitzinger, 1856. *Zootaxa* 3947:30–48.
688
689 Castro MC, Ribeiro AM, Ferigolo J, Langer MC. 2013. Redescription of *Dasypus punctatus*
690 Lund, 1840 and considerations on the genus *Propraopus* Ameghino, 1881 (Xenarthra,
691 Cingulata). *Journal of Vertebrate Paleontology* 33(2):434-447.
692
693 Ciancio MR, Castro MC, Asher RJ. 2012. Evolutionary implications of dental eruption in
694 *Dasypus* (Xenarthra). *Journal of Mammalian Evolution* 19:1–8.
695
696 Curtis A, Van Valkenburgh B. 2014. Beyond the sniffer: frontal sinuses in Carnivora. *The*
697 *Anatomical Record* 297:2047-2064.
698
699 Curtis A, Lai G, Wei F, Van Valkenburgh B. 2015. Repeated Loss of Frontal Sinuses in Arctoid
700 Carnivorans. *Journal of Morphology* 276:22–32.
701
702 Cuvier G. 1845. *Leçons d'anatomie comparée de Georges Cuvier, recueillies et publiées par M.*
703 *Duméril, 2nde édition. Tome troisième contenant le système nerveux et les organes des sens*.
704 Paris : Fortin, Masson et Cie. 760 pp.

Delsuc F, Gibb GC, Kuch M, Billet G, Hautier L, Southon J, Rouillard J-M, Fernicola JC, Vizcaino SF, MacPhee RDE, Poinar HN. 2016. The phylogenetic affinities of the extinct glyptodonts. *Current Biology* 26:R141–R156.

Edinger T. 1950. Frontal sinus evolution (particularly in the Equidae). *Bulletin of the Museum of Comparative Zoology at Harvard College* 103:411–496.

Farke AA. 2010. Evolution and functional morphology of the frontal sinuses in Bovidae (Mammalia: Artiodactyla), and implications for the evolution of cranial pneumaticity. *Zoological Journal of the Linnean Society* 159:988–1014.

Feijo A, Cordeiro-Estrela P. 2016. Taxonomic revision of the *Dasypus kappleri* complex, with revalidations of *Dasypus pastasae* (Thomas, 1901) and *Dasypus beniensis* Lönnberg, 1942 (Cingulata, Dasypodidae). *Zootaxa* 4170(2):271–297.

Fernicola JC, Toledo N, Bargo S, Vizcaino S. 2012. A neomorphic ossification of the nasal cartilages and the structure of paranasal sinus system of the glyptodont *Neosclerocalyptus* Paula Couto 1957 (Mammalia, Xenarthra). *Paleontologia Electronica* 15(3):1-22.

Foster FR, Shapiro DF. 2016. Convergent loss of paranasal sinuses in mammals is explained by their deleterious effects on high-frequency communications. *The Anatomical Record* 299: 133.

728 Gibb GC, Condamine FL, Kuch M, Enk J, Moraes-Barros N, Superina M, Poinar HN, Delsuc F.
729 2016. Shotgun mitogenomics provides a reference phylogenetic framework and timescale for
730 living xenarthrans. *Molecular Biology and Evolution* 33(3):621–642.
731
732 Hallgrímsson B, Hall BK. 2005. Variation and variability: central concepts in biology. In:
733 Hallgrímsson B, Hall BK, eds. *Variation: A central concept in Biology*. Cambridge: Elsevier
734 Academic Press, 1-7.
735
736 Hamlett GWD. 1939. Identity of *Dasypus septemcinctus* Linnaeus with notes on some related
737 species. *Journal of Mammalogy* 20:328-336.
738
739 Hooper ET. 1947. Notes on Mexican mammals. *Journal of Mammalogy* 28:40.
740
741 Huchon D, Delsuc F, Catzeflis FM, Douzery EJP. 1999. Armadillos exhibit less genetic
742 polymorphism in North America than in South America: nuclear and mitochondrial data confirm
743 a founder effect in *Dasypus novemcinctus* (Xenarthra). *Molecular Ecology* 8:1743–1748.
744
745 Ito T, Nishimura TD. 2016. Enigmatic diversity of the maxillary sinus in macaques and its
746 possible role as a spatial compromise in craniofacial modifications. *Evolutionary Biology*
747 43:414–426.
748
749 Ito T, Kawamoto Y, Hamada Y, Nishimura TD. 2015. Maxillary sinus variation in hybrid
750 macaques: implications for the genetic basis of craniofacial pneumatization. *Biological*

751 *Journal of the Linnean Society* 115(2):333–347.

752

753 Kim DI, Lee U, Park SO, Kwak DS, Han SH. 2013. Identification Using Frontal Sinus by
754 Three-Dimensional Reconstruction from Computed Tomography. *Journal of Forensic Sciences*
755 58(1):5-12.

756

757 Klingenberg CP. 2010. Evolution and development of shape: integrating quantitative approaches.
758 *Nature Reviews Genetics* 11(9):623-635.

759

760 Krentzel D, Angielczyk K. 2016. Evolution, development and function of the elaborate frontal
761 sinuses in porcupines. *The Anatomical Record* 299:148.

762

763 Lönnberg E. 1913. Mammals from Ecuador and related forms. *Arkiv för Zoologi* 8:1-36.

764

765 Maier W. 2000. Ontogeny of the nasal capsule in cercopithecoids: a contribution to the
766 comparative and evolutionary morphology of catarrhines. In: Whitehead PF, Jolly CJ, eds. *Old*
767 *World Monkeys*. Cambridge: University Press, 99–132.

768

769 Maier W, Ruf I. 2014. Morphology of the nasal capsule of Primates – with special reference to
770 *Daubentonia* and *Homo*. *The Anatomical Record* 297:1985–2006.

771

772 Macrini TE. 2012. Comparative morphology of the internal nasal skeleton of adult marsupials
773 based on X-ray computed tomography. *Bulletin of the American Museum of Natural History*
774 365:1-91.
775
776 Marquez S. 2008. The paranasal sinuses: the last frontier in craniofacial biology. *The Anatomical*
777 *Record* 291:1350–1361.
778
779 McBee K, Baker RJ. 1982. *Dasypus novemcinctus*. *Mammalian Species* 162:1-9.
780
781 McDonough CM, Loughry WJ. 2013. The nine-banded armadillo: a natural history. Norman,
782 OK: University of Oklahoma Press, 323 pp.
783
784 Mondolfi E. 1968. Descripción de un nuevo armadillo del genero *Dasypus* de Venezuela
785 (Mammalia - Edentata). *Memoria de la sociedad de ciencias naturales La Salle* 27:149-167.
786
787 Moraes-Barros N, Arteaga MC. 2015. Genetic diversity in Xenarthra and its relevance to patterns
788 of neotropical biodiversity. Journal of Mammalogy 96(4):690–702.
789
790 Nomina Anatomica Veterinaria, 5th edn. 2005. Hannover, Columbia, Gent, Sapporo: Editorial
791 Committee. Available at: http://www.wava-amav.org/downloads/nav_2005.pdf.
792

793 Novacek MJ. 1993. Patterns of diversity in the mammalian skull. In: Hanken J, Hall BK, eds.
794 *The Skull, Volume 2: Patterns of Structural and Systematic Diversity.* Chicago: University of
795 Chicago Press, pp. 438-545.
796
797 Paulli S. 1900a. Über die Pneumaticität des Schädels bei den Säugerthieren. Eine
798 morphologische Studie. II. Über die Morphologie des Siebbeins und die der Pneumaticität bei
799 den Ungulaten und Probosciden. *Gegenbaurs Morphologisches Jahrbuch* 28:179–251.
800
801 Paulli S. 1900b. Über die Pneumaticität des Schädels bei den Säugerthieren. Eine
802 morphologische Studie. III. Über die Morphologie des Siebbeins und die der Pneumaticität bei
803 den Insectivoren, Hyracoideen, Chiropteren, Carnivoren, Pinnipedien, Edentaten, Rodentiern,
804 Prosimiern und Primaten. *Gegenbaurs Morphologisches Jahrbuch* 28:483-564.
805
806 Peters W. 1864. Ueber neue Arten der Saugethier-gattungen *Geomys*, *Haplodon* und *Dasypus*.
807 *Monatsbericht der Königlich-Preussischen Akademie der Wissenschaften zu Berlin* 1865: 177–
808 181.
809
810 Reinbach W. 1952a. Zur Entwicklung des Primordialcraniums von *Dasypus novemcinctus* Linné
811 (*Tatusia novemcincta* Lesson). Teil 1. *Zeitschrift für Morphologie und Anthropologie* 44: 375-
812 444.
813

814 Reinbach W. 1952b. Zur Entwicklung des Primordialcraniums von *Dasypus novemcinctus* Linné
815 (*Tatusia novemcincta* Lesson). Teil 2. *Zeitschrift für Morphologie und Anthropologie,* Teil 2: Z.
816 Morph. Anthrop. 45: 1-72.
817
818 Rossie JB. 2006. Ontogeny and homology of the paranasal sinuses in Platyrrhini (Mammalia:
819 Primates). *Journal of Morphology* 267:1–40.
820
821 Rossie JB. 2008. The phylogenetic significance of anthropoid paranasal sinuses. *The Anatomical*
822 *Record* 291:1485–1498.
823
824 Ruf I. 2014. Comparative anatomy and systematic implications of the turbinal skeleton in
825 Lagomorpha (Mammalia). *The Anatomical Record* 297:2031–2046.
826
827 Russell RJ. 1953. Description of a new armadillo (*Dasypus novemcinctus*) from Mexico with
828 remarks on geographic variation of the species. *Proceedings of the Biological Society of*
829 *Washington* 66:21.
830
831 Sharp AC. 2016. A quantitative comparative analysis of the size of the frontoparietal sinuses and
832 brain in vombatiform marsupials. *Memoirs of Museum Victoria* 74:331–342.
833
834 Sharp AC, Rich TH. 2016. Cranial biomechanics, bite force and function of the endocranial
835 sinuses in Diprotodon optatum, the largest known marsupial. *Journal of Anatomy* 228:984-995.
836

837 Slavec ZZ. 2005. Identification of family relationships by epigenetic traits. *Anthropologischer*
838 *Anzeiger* 63(4):401-408.
839
840 Smith TD, Rossie JB, Cooper GM, Mooney MP, Siegel MI. 2005. Secondary pneumatization of
841 the maxillary sinus in callitrichid primates: insights from immunohistochemistry and bone cell
842 distribution. *The Anatomical Record Part A: Discoveries in Molecular, Cellular, and*
843 *Evolutionary Biology* 285(2):677-89.
844
845 Soares da Silva AB, de Sousa Cavalcante MMA, Araújo JVS, de Oliveira IM, Fonseca CMB,
846 dos Santos Rizzo M, de Carvalho MAM, Júnior AMC. 2016. Anatomy of the nasal cavity of
847 nine-banded armadillo (*Dasypus novemcinctus*, Linnaeus, 1758). *Jornal Interdisciplinar de*
848 *Biociências* 1:1-4.
849
850 Szilvássy J. 1982. Zur Variation, Entwicklung und Vererbung der Stirnhöhlen. *Annalen des*
851 *Naturhistorischen Museums in Wien. Serie A für Mineralogie undPetrographie, Geologie und*
852 *Paläontologie, Anthropologie und Prähistorie*, 84:97-125.
853
854 Tanner JB, Dumont ER, Sakai ST, Lundrigan BL, Holekamp KE. 2008. Of arcs and vaults: the
855 biomechanics of bonecracking in spotted hyenas (*Crocuta crocuta*). *Biological Journal of the*
856 *Linnean Society* 95:246–255.
857
858 Van Valen L. 1962. A study of fluctuating asymmetry. *Evolution* 16(2):125-142.
859

Van Valkenburgh B, Smith TD, Craven BA. 2014. Tour of a labyrinth: exploring the vertebrate nose. *The Anatomical Record* 297:1975–1984.

Weidenreich F. 1941. The brain and its role in the phylogenetic transformation of the human skull. *Transactions of the American Philosophical Society* 31:320–442.

Weinert H. 1925. Die Ausbildung der Stirnhohlen als stammesgeschichtliches Merkmal. Eine vergleichend-anatomische Studie mit einem Atlas der Stirnhohlen und einem neuen Meftzirkel zur Ermittelung der inneren Schadelmafie. *Zeitschrift für Morphologie und Anthropologie* 25(2): 243-357.

Wetzel RM, Gardner AL, Redford KH, Eisenberg JF. 2008. Order Cingulata Illiger, 1811. In: Gardner AL, ed. *Mammals of South America, volume 1: marsupials, xenarthrans, shrews and bats*. Chicago: University of Chicago Press, pp. 128-157.

Wible JR, Gaudin TJ. 2004. On the cranial osteology of the yellow armadillo *Euphractus sexcinctus* (Dasypodidae, Xenarthra, Placentalia). *Annals of Carneggie Museum* 73(3):117-196.

Witmer LM. 1997. The evolution of the antorbital cavity of archosaurs: a study in soft-tissue reconstruction in the fossil record with an analysis of the function of pneumaticity. *Journal of Vertebrate Paleontology* 17:1–73.

882 Witmer LM. 1999. The Phylogenetic History of Paranasal Air Sinuses. In: Koppe T, Nagai H,
883 Alt KW, eds. *The paranasal sinuses of higher primates: development, function and evolution*.
884 Berlin: Quintessence, pp. 21-34.
885
886 Zollikofer CPE, Weissmann JD. 2008. A morphogenetic model of cranial pneumatization based
887 on the invasive tissue hypothesis. *The Anatomical Record* 291:1446–1454.
888
889 Zuckerkandl E. 1887. *Das periphere Geruchsorgan der Säugethiere: eine vergleichend*
890 *anatomische Studie*. Whitefish: Kessinger Publishing, 146pp.
891
892
893

894 Figure legends

895 **Figure 1**. Dorsal views of virtually reconstructed skulls of long-nosed armadillos species, with
896 bone transparency showing internal paranasal sinuses and recesses in light blue. A-C, *D.*
897 *novemcinctus*; D, *D. pilosus*; E, *D. hybridus*; F, *D. septemcinctus*; G, *D. kappleri*. See Material
898 and Methods for the abbreviations. Scale-bar: 10mm.
899
900 **Figure 2.** Paranasal sinuses and recesses in juvenile individuals of *Dasypus novemcinctus*,
901 virtual reconstructions of skulls in lateral (A, C, E) and dorsal views (B, D, F), with and without
902 bone transparency. See Material and Methods for the abbreviations. Scale-bar: 10mm.
903

Figure 3. Virtual reconstruction of the skull of the stillborn specimen AMNH 33150, *Dasypus novemcinctus*, with bone transparency leaving the caudal maxillary recess and cavity for the frontal diploic vein apparent. A, dorsal view; B, lateral view.

Figure 4. Dorsal views of virtually reconstructed skulls of adult specimens of *Dasypus novemcinctus* clustered by morphotypes of paranasal anatomy as described in the text. A-F, northern morphotype; G-L, southern morphotype; M-P, Guianan morphotype; Q-R, problematic specimens (see text). Bone transparency leaves apparent the paranasal recesses and sinuses in light blue. Scale bar: 10 mm.

Figure 5. μCT transversal slices through the skull of *D. novemcinctus* individuals showing details of the internal paranasal anatomy for each morphotype (A, northern; B, southern; C, Guianan). Slices were made at similar transversal locations at the posterior end of the anterior root of the zygomatic arch. See Material and Methods for the abbreviations. Scale-bar: 10mm.

Figure 6. Summary map showing the geographical distribution of nine-banded armadillo specimens (*Dasypus novemcinctus*) investigated in this study and their attribution to a paranasal morphotype. Each morphotype is represented by a schematic dorsal view of skulls (in grey) on which the paranasal sinuses and recesses are drawn (in blue, yellow, or green for each morphotype). Specimens reported with a star denote the absence of geographical information besides the country of origin.

927

928

Figure 1

Figure 1. Dorsal views of virtually reconstructed Dasypus skulls with internal paranasal sinuses

Dorsal views of virtually reconstructed skulls of long-nosed armadillos species, with bone transparency showing internal paranasal sinuses and recesses in light blue. A-C, *D. novemcinctus*; D, *D. pilosus*; E, *D. hybridus*; F, *D. septemcinctus*; G, *D. kappleri*. See Material and Methods for the abbreviations. Scale-bar: 10mm.

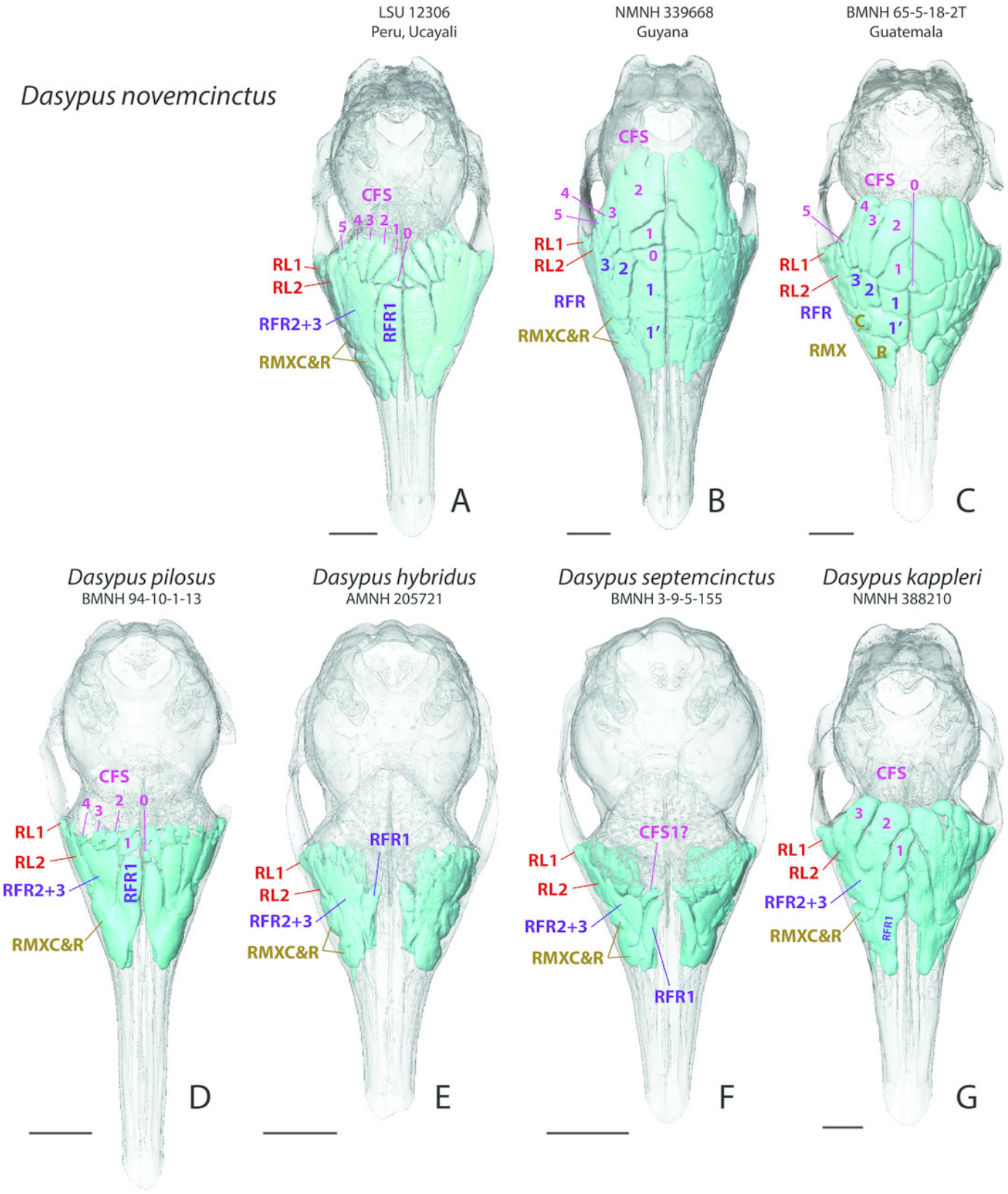
Dasypus novemcinctus
LSU 12306
Peru, Ucayali
NMNH 339668
Guyana
BMNH 65-5-18-2T
Guatemala
CFS
RL1
RL2
RFR2+3
RFR1
RMXC&R
RFR
RMX
A
B
C
Dasypus pilosus
BMNH 94-10-1-13
Dasypus hybridus
AMNH 205721
Dasypus septemcinctus
BMNH 3-9-5-155
Dasypus kappleri
NMNH 388210
CFS1?
D
E
F
G

Figure 2

Figure 2. Paranasal sinuses and recesses in juvenile individuals of *Dasypus novemcinctus*

Paranasal sinuses and recesses in juvenile individuals of *Dasypus novemcinctus*, virtual reconstructions of skulls in lateral (A, C, E) and dorsal views (B, D, F), with and without bone transparency. See Material and Methods for the abbreviations. Scale-bar: 10mm.

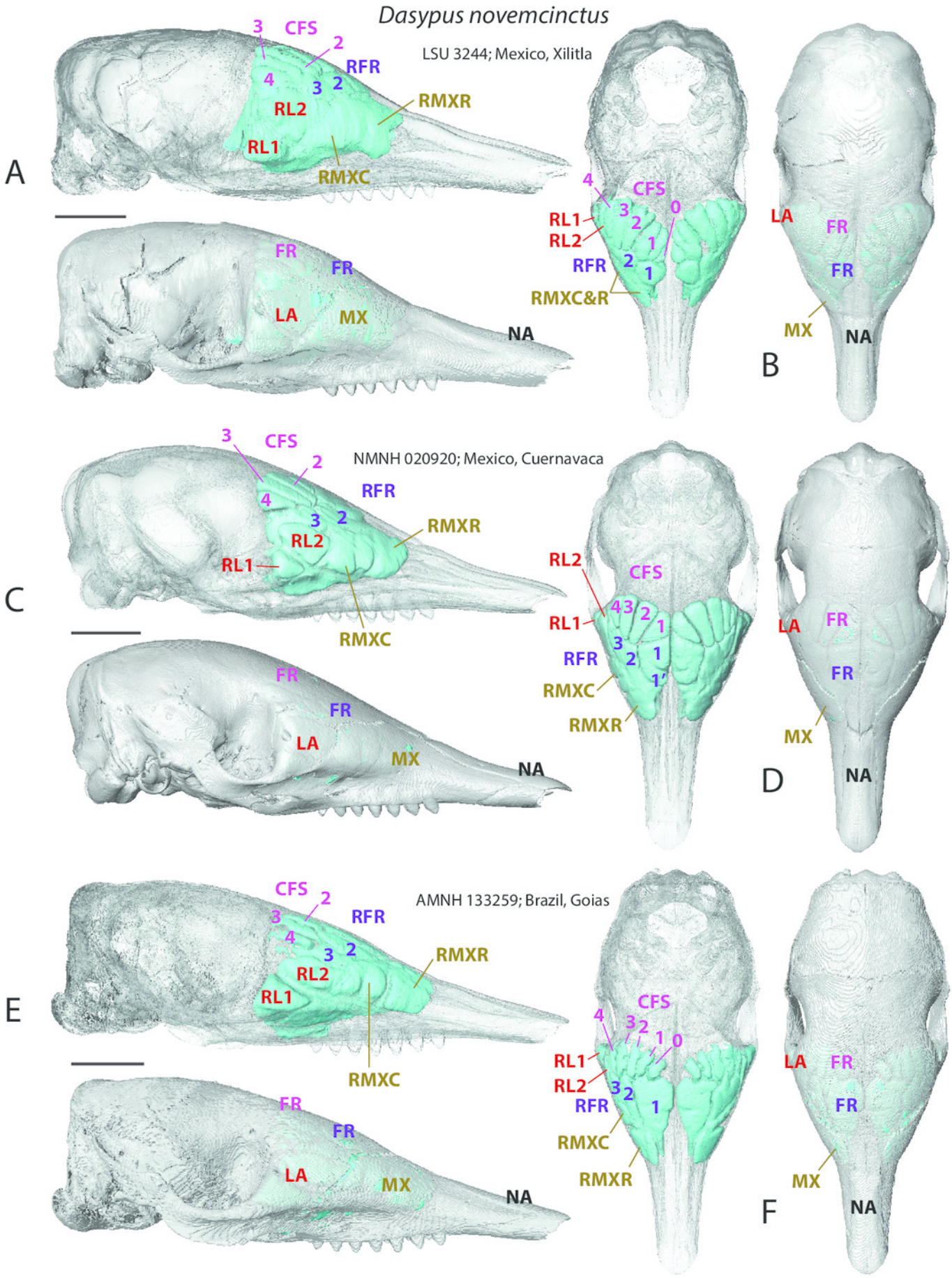
Dasypus novemcinctus
LSU 3244; Mexico, Xilitla
NMNH 020920; Mexico, Cuernavaca
AMNH 133259; Brazil, Goias
A
B
C
D
E
F
CFS
RFR
RMXR
RMXC
RL1
RL2
RMXC&R
FR
LA
MX
NA

Figure 3

Figure 3. Virtual reconstruction of the skull of the stillborn specimen AMNH 33150, *Dasypus novemcinctus*

Virtual reconstruction of the skull of the stillborn specimen AMNH 33150, *Dasypus novemcinctus*, with bone transparency leaving the caudal maxillary recess and cavity for the frontal diploic vein apparent. A, dorsal view; B, lateral view.

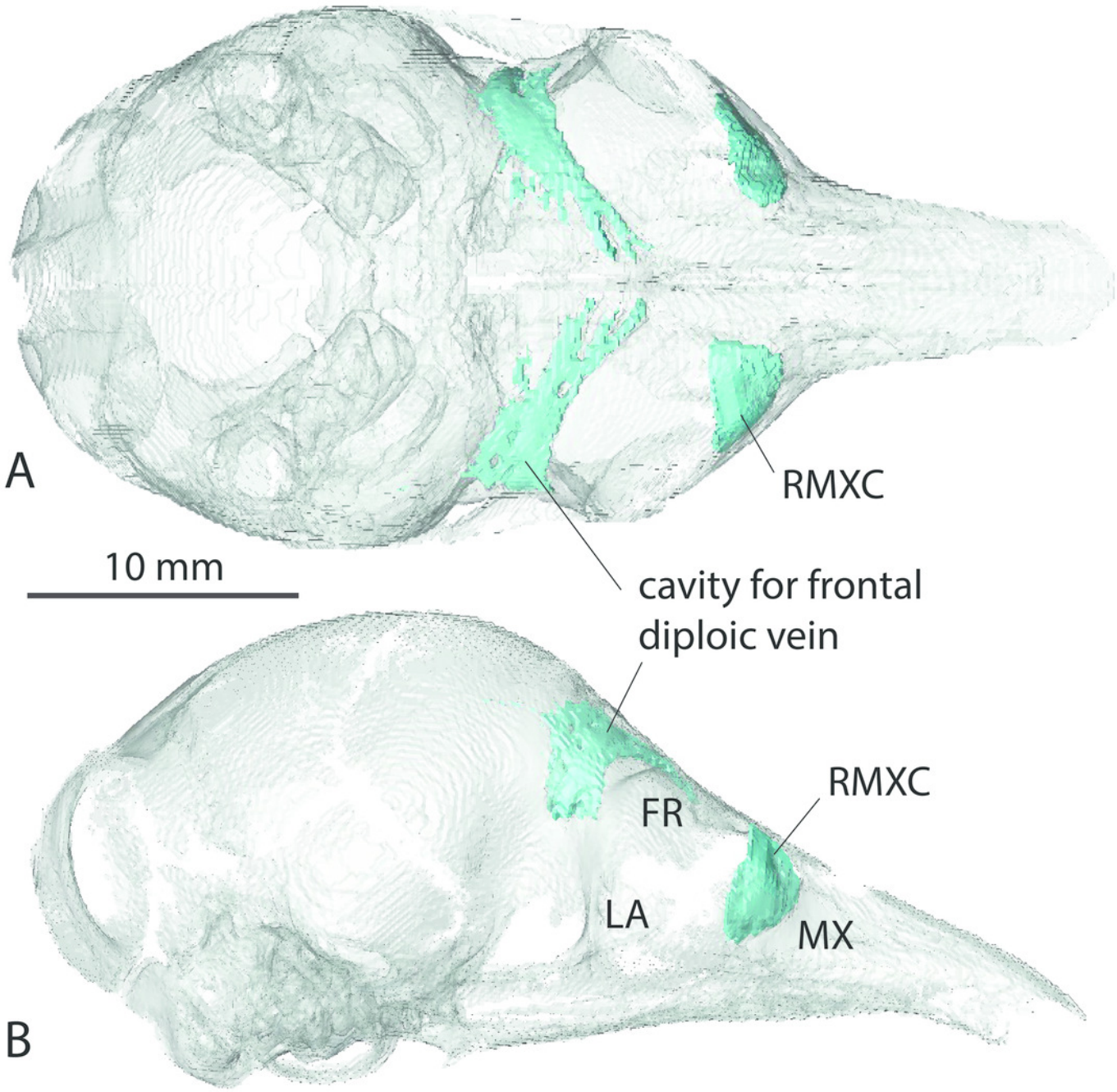
A
RMXC
10 mm
cavity for frontal
diploic vein
RMXC
FR
LA
MX
B

Figure 4

Figure 4. Dorsal views of virtually reconstructed skulls of adult specimens of *Dasypus novemcinctus* clustered by morphotypes of paranasal anatomy as described in the text.

A-F, northern morphotype; G-L, southern morphotype; M-P, Guianan morphotype; Q-R, problematic specimens (see text). Bone transparency leaves apparent the paranasal recesses and sinuses in light blue. Scale bar: 10 mm.

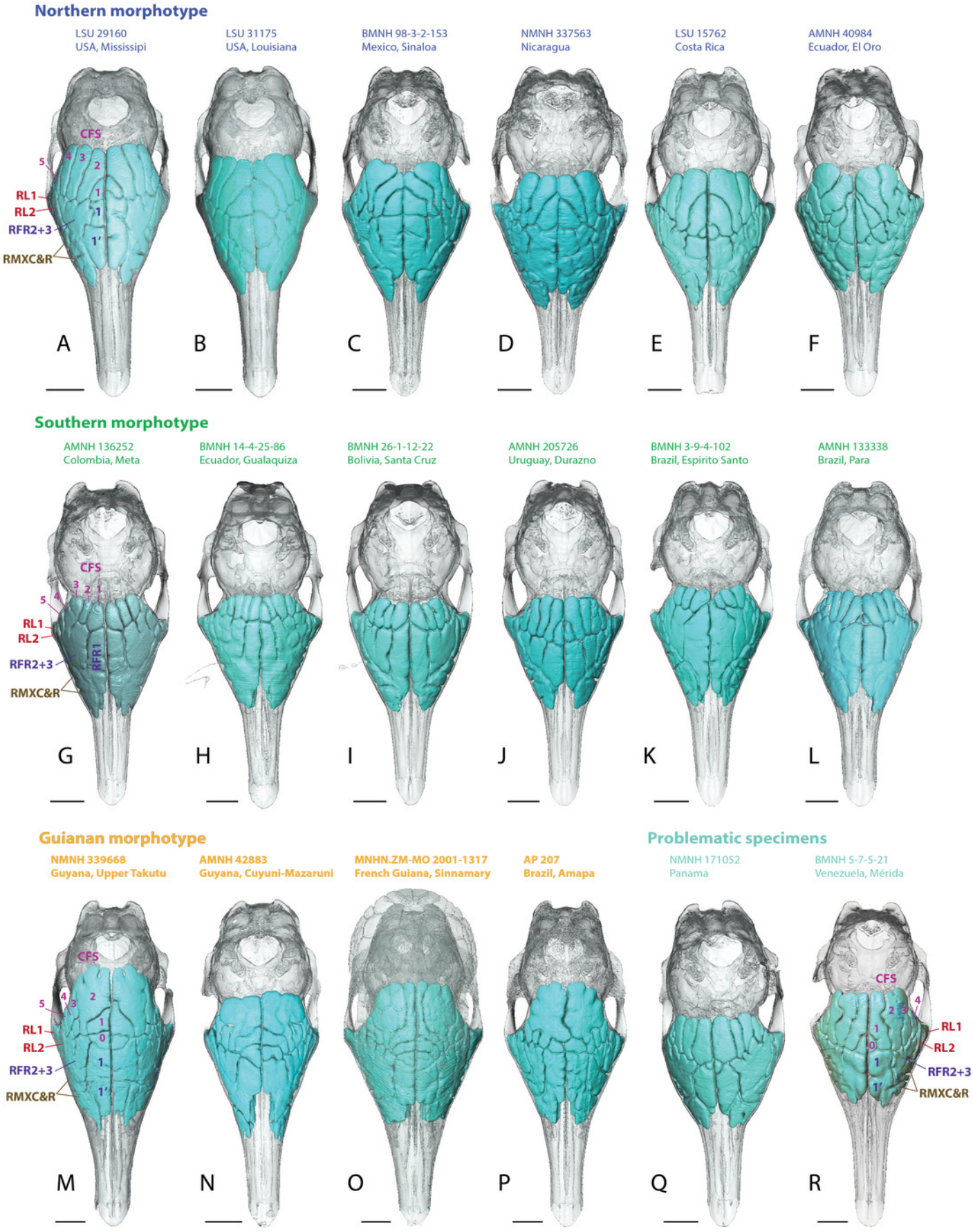
Northern morphotype
LSU 29160
USA, Mississipi
LSU 31175
USA, Louisiana
BMNH 98-3-2-153
Mexico, Sinaloa
NMNH 337563
Nicaragua
LSU 15762
Costa Rica
AMNH 40984
Ecuador, El Oro
CFS
RL1
RL2
RFR2+3
RMXC&R
A
B
C
D
E
F
Southern morphotype
AMNH 136252
Colombia, Meta
BMNH 14-4-25-86
Ecuador, Gualaquiza
BMNH 26-1-12-22
Bolivia, Santa Cruz
AMNH 205726
Uruguay, Durazno
BMNH 3-9-4-102
Brazil, Espirito Santo
AMNH 133338
Brazil, Para
RFR1
G
H
I
J
K
L
Guianan morphotype
NMNH 339668
Guyana, Upper Takutu
AMNH 42883
Guyana, Cuyuni-Mazaruni
MNHN.ZM-MO 2001-1317
French Guiana, Sinnamary
AP 207
Brazil, Amapa
Problematic specimens
NMNH 171052
Panama
BMNH 5-7-5-21
Venezuela, Mérida
M
N
O
P
Q
R

Figure 5

Figure 5. µCT transversal slices through the skull of *D. novemcinctus* individuals showing details of the internal paranasal anatomy for each morphotype (A, northern; B, southern; C, Guianan).

Slices were made at similar transversal locations at the posterior end of the anterior root of the zygomatic arch. See Material and Methods for the abbreviations. Scale-bar: 10mm.

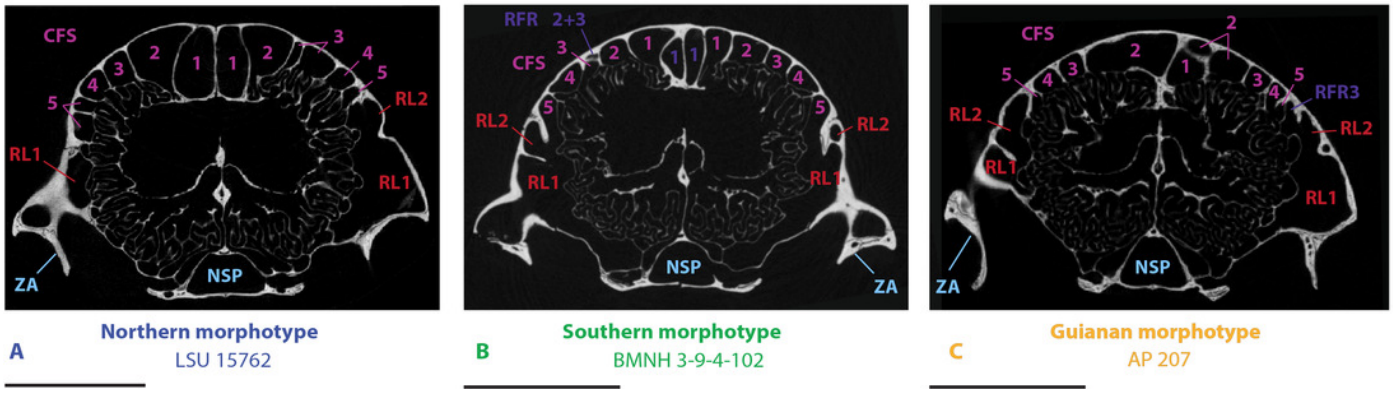

Figure 6

Figure 6. Summary map showing the geographical distribution of nine-banded armadillo specimens (*Dasypus novemcinctus*) investigated in this study and their attribution to a paranasal morphotype.

Each morphotype is represented by a schematic dorsal view of skulls (in grey) on which the paranasal sinuses and recesses are drawn (in blue, yellow, or green for each morphotype). Specimens reported with a star denote the absence of geographical information besides the country of origin.

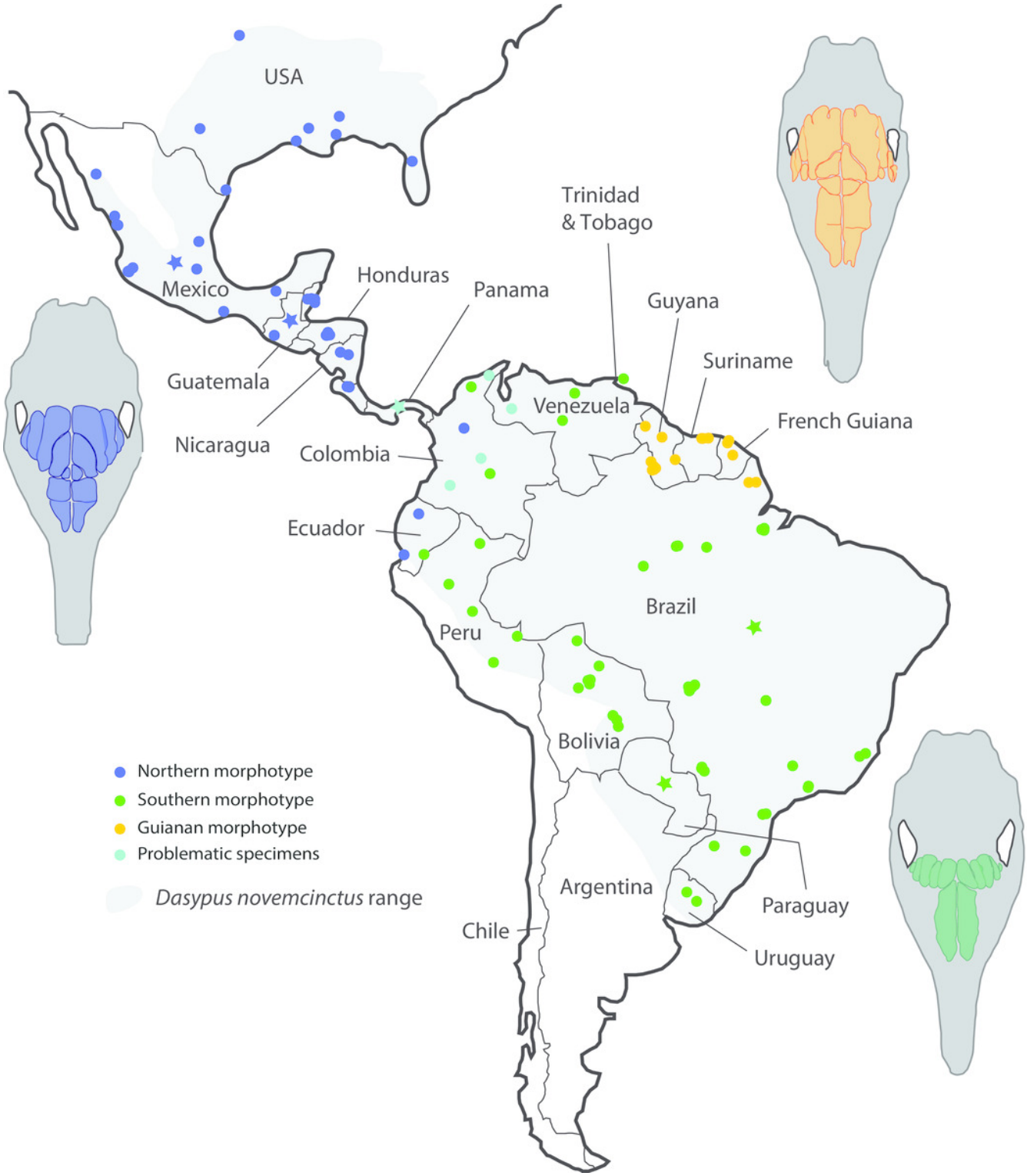
USA
Mexico
Honduras
Panama
Trinidad
& Tobago
Guyana
Suriname
French Guiana
Venezuela
Guatemala
Nicaragua
Colombia
Ecuador
Brazil
Peru
Bolivia
Argentina
Paraguay
Chile
Uruguay
Northern morphotype
Southern morphotype
Guianan morphotype
Problematic specimens
Dasypus novemcinctus range